Spectroscopic Study and Simulation from Recent Structural Models for Eumelanin: II. Oligomers

Klaus B. Stark*

Accelrys, Incorporated, 9685 Scranton Road, San Diego, California 92121-3752

James M. Gallas

Department of Physics and Astronomy, University of Texas at San Antonio, San Antonio, Texas 78249

Gerry W. Zajac

BP Research Center, P.O. Box 3011, Naperville, Illinois 60566-7011

Melvin Eisner

Department of Physics, University of Houston, Houston, Texas 77204

Joseph T. Golab

BP Research Center, P.O. Box 3011, Naperville, Illinois 60566-7011

Received: April 10, 2003; In Final Form: July 25, 2003

Spectroscopic simulations of a leading structural model for melanin, which is the pigment responsible for coloration and photo protection in humans and animals, were conducted. In direct continuation of an earlier study on possible monomer and dimer subunits of eumelanin, we have performed density functional theory (DFT) calculations on a recent structural model for eumelanin based on higher oligomers of neutral 5,6-indolequinone. This paper further reports on our semiempirical spectroscopic simulations for the higher oligomer (tetramers through hexamers) energy-minimized structures. A linear combination of the oligomeric spectra reproduces several features of the experimental spectrum. This result strongly supports the assumption that melanin is constituted of substructures such as those considered in this study.

1. Introduction

Melanin pigments form a class of biological polymers that provide coloration and photoprotection to animals and plants.[1−3] Melanin is found in the skin,[3] inner ear,[4] the mid-brain,[5] and in the iris and retinal pigment epithelium and choroids.[6] Its sunlight protective function being long established by numerous scientific investigations,[7] melanin may perform other biological functions in significant diseases such as Parkinson's disease and age-related macular degeneration.[8−11]

Melanins are roughly classified into three classes:[12] (i) eumelanins, which are black and dark-brown nitrogen-containing pigments; (ii) sulfur-containing phaeomelanin pigments, which result in coloration such as red hair; and (iii) plant phila pigments that are called allomelanins. We will restrict this discussion to the eumelanins.

As a photoprotective light filter, melanin must absorb light in a manner that should reflect extensive refinement from evolution. Presumably, this fine tuning should be manifested in the optical absorption spectrum. This spectrum of melanin is characterized by a monotonically increasing function of the photon energy over a large portion of the solar spectrum spanning the near-IR into the visible, where the absorption increases in an approximately exponential manner between wavelengths of 700 and 200 nm (Figure 1). In the spectrum for a tyrosine-synthesized eumelanin, two absorption shoulders appear: at ∼340 nm and ∼220−240 nm. A very similar spectrum for eumelanin has been published previously, indicating soft absorption shoulders in these spectral regions.[13]

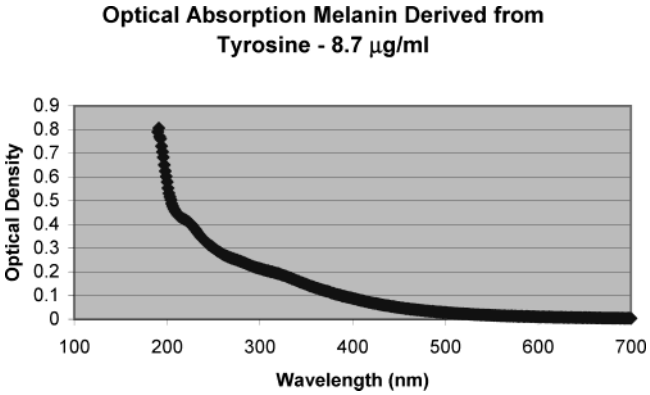

Figure 1. Experimental absorption spectrum of melanin derived from tyrosine that was obtained by one of the authors (J.MG.); the tyrosine used in the measurement was balanced with deionized water on both the reference and the sample cell.

An understanding of the basis for the optical absorption of melanin is an intriguing and challenging goal. However, the absorption spectrum is not yet understood, largely because the melanin structure itself has been unknown.

* Corresponding author. E-mail: kstark@accelrys.com.

10.1021/jp034965r CCC: $25.00
Published on Web 09/24/2003

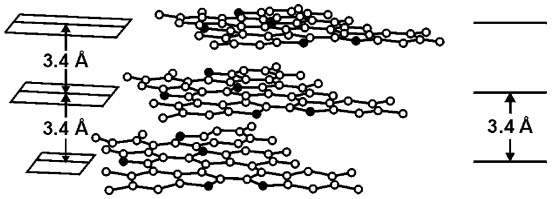

Figure 2. Schematic representation of a melanin protomolecule. Five to seven monomers of 5−6 indole quinone (IQ) are arranged in a plane, forming 3−4 layers that are stacked 3.4 Å apart. The white circles in the framework represent C atoms, and the dark circles represent N atoms. The quinone O atoms are also represented as white circles, and the H atoms are not represented. (Figure taken with kind permission from ref 17.)

Although there has been little understanding of melanin morphology, structure, and even size, there has been some agreement regarding the molecular units that comprise the polymerized structure. Typical units include dihydroxyindole (DHI), dihydroxyindole−carboxylic acid (DHICA), and 5,6-indolequinone (IQ). Early molecular orbital calculations[14] on monomer units predicted molecular properties, such as electron donor and acceptor qualities, in accord with experimental data known for the polymer.

More recently, Bolivar-Martinez et al.[15] performed ab initio and semiempirical calculations on different monomers, IQ and the reduced forms, semiquinone (SQ), and hydroquinone (HQ). Calculations were both performed for the neutral molecules and for singly and doubly charged anions. Although some connection with the optical absorption spectra of eumelanins was referenced, these calculations were also only based on monomeric units.

However, recent wide-angle X-ray scattering studies (WAXS),[16,17] scanning tunneling microscopy (STM),[18−20] and small-angle X-ray scattering (SAXS)[21] experiments have revealed both short-range structure and stacking features of nanometer-sized melanins in aqueous media.

These results have led to the proposal of a proto-molecule for melanin, consisting of covalently bonded monomers of 5,6-indolequinone to form single sheets with lateral extents of 15−20 Å (Figure 2). Three or four sheets are stacked with spacings of 3.4 Å.

The current work is a first attempt to re-examine the nature of the optical absorption spectrum, in terms of more-specific nonstacked structures. The effect of stacking will be addressed in a future publication.[22] The intent of this work is to perform molecular orbital calculations on oligomer structures, thereby providing electronic wave functions from which optical spectra may be derived.

Although melanin seems to be an aggregated particle, it has a substructure that consists of covalently bonded planar sheets. In this paper, we will assume, as a starting point, that the optical properties of the individual sheets are largely unchanged when they are stacked. One can anticipate that some broadening or a shift toward longer wavelength absorption will occur when aggregation to larger particles happens.

In the first portion of our studies (Part I),[23] we provided density functional theory (DFT) calculations on the monomer of neutral 5,6-indolequinone and its reduced forms, semiquinone and hydroquinone. Five possible dimers of the DHI units were also considered and optimized. From the optimized structures, absorption spectra for these structures were calculated using configuration interaction (CI) schemes and a semiempirical Hamiltonian. The results of this work indicated sufficient agreement with earlier theoretical work[15] and sufficient correspondence with published experimental work[24] to warrant an extension of the methodology to include the higher oligomeric units that are believed to represent the molecular structure of eumelanins.

This second part of our spectroscopic studies furthers the same approach to the higher oligomers (tetramers through hexamers) and examines the possibility that the combined absorption spectra of the oligomeric units tend to converge to the spectrum of eumelanin.

2. Calculational Details

All structure optimizations were performed using Accelrys's DFT program DMol^3.[25,26] DMol^3 utilizes a basis set of numeric atomic functions that are exact solutions to the Kohn−Sham equations for the atoms.[27] These basis sets are generally more complete than a comparable set of linearly independent Gaussian functions and have been demonstrated to have small basis set superposition errors.[27] In the present study, a polarized split valence basis set, which is termed a double numeric polarized (DNP) basis set, has been used. All structure optimizations have been performed using the nonlocal BP[28−30] functional.

Atom-centered grids were used for the numerical integration. The particular grid used ~1000 grid points for each atom in the calculation and corresponds to the "Medium" option in DMol^3.[31] A real space cutoff of 4 was used for the numerical integration.

All self-consistent field (SCF) calculations were converged to a root-mean-square (rms) change in the charge density of $<1 \times 10^{-5}$ Hartree (hereafter, the unit Hartree will be abbreviated as Ha). Geometries were optimized using analytic gradients and an efficient algorithm that used delocalized internal coordinates.[32−34] Geometries were optimized so that the change of energy was $<2 \times 10^{-5}$ Ha, and the change of the maximum force on the atoms was <0.004 Ha/Å.

On the DFT optimized structures, absorption spectra have been calculated, using the Pair Excitation Configuration Interaction (PECI) method[35,36] and the AM1 Hamiltonian,[37] as implemented in the semiempirical program VAMP[38] that is available from Accelrys, Inc. In the PECI method, excited states are calculated by including all single and double excitations in which a complete electron pair is promoted. This is a very economical and effective CI expansion for closed-shell molecules and is used in the VAMP program for the calculation of spectra or hyperpolarizabilities. In the current calculations, eight orbitals have been included in the PECI expansion.

3. Results

The results of the geometry optimizations of the monomer and dimer structures[23] have shown that the structures predicted by the local density approximation (LDA) and the generalized gradient approximation (GGA) optimizations are, in principle, very similar. However, for weak interactions such as hydrogen bonding, the LDA calculations on the dimers[23] predicted bond lengths that were too short, reflecting the well-known tendency of LDA to overbind.[39−41] Because hydrogen bonding interactions also occur in the higher oligomers, all structure optimizations have been performed on the DFT/BP/DNP level. The resulting geometries for possible tetramer, pentamer, and hexamer structures are displayed in Figure 3.

The tetramer structure (Figure 3a) is predicted to be almost planar: only one of the quinone six-membered rings is slightly twisted out of the plane (as observed in the back portion of Figure 3a). This twist is mostly due to the repulsion of the carbonyl atoms in two adjacent six-membered rings, which force the O atom to assume positions above and below the plane

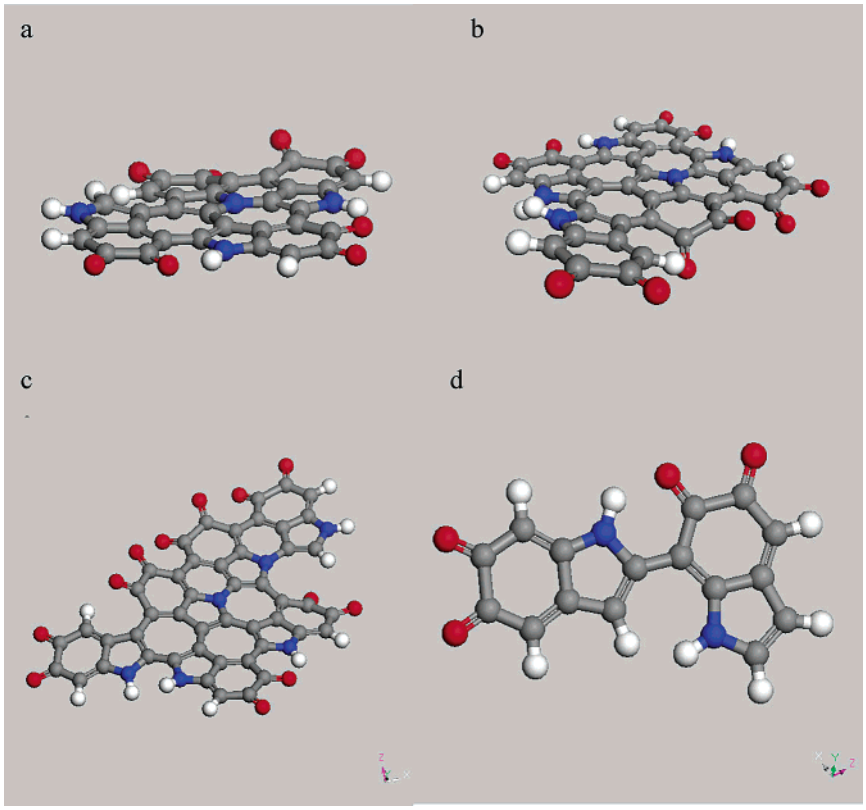

Figure 3. DFT-optimized oligomer structures ((a) tetramer, (b) pentamer, and (c) hexamer); the most-stable dimer structure from ref 23 is depicted in panel d. C atoms are displayed in gray, O atoms in red, N atoms in blue, and H atoms in white.

defined by the backbone of the oligomer. The H atoms of the indole N and adjacent O atoms generally form hydrogen bonds. In the tetramer, two hydrogen bonds are formed, with bond lengths of 1.69 and 1.86 Å, respectively. Hydrogen bonds generally occur when the indole quinone subunits are fused, such as that in Dimer 3, which is the most stable of the possible dimer structures[23] (see Figure 3d). The second hydrogen bond formed in the tetramer (Figure 3a, right) is weaker, because the indole N atom belongs to the slightly distorted substructure of the molecule, which is formed due to the repulsion between the adjacent carbonyl O atoms.

The same general remarks about the structure can be made for the pentamer (Figure 3b) and the hexamer (Figure 3c) structures. Two hydrogen bonds very similar to those in the tetramer are found in the pentamer structure. The bond lengths of these hydrogen bonds are 1.67 and 1.84 Å, respectively. In the pentamer, a third hydrogen bond between a H atom of one quinoline six-membered ring and the adjacent carbonyl O atom of a second quinoline substructure (Figure 3b, bottom right) is weaker ($r = 2.15$ Å) than the former hydrogen bonds. This is due to the aforementioned repulsion of the neighboring carbonyl O atom, which moves them above and below the plane of the oligomer backbone and, thus, makes the hydrogen-bonded interaction less attractive.

The hexamer (Figure 3c) shows the largest deviation from planarity. Here, two hydrogen bond interactions are found: (i) a strong N−H interaction ($r = 1.69$ Å) of the type found in the tetramer (to the right of Figure 3c) and (ii) a weak O−H interaction ($r = 2.19$ Å) of the type found in the pentamer (to the left of Figure 3c).

Binding energies for the oligomers are reported in Table 1. The total binding energy has been divided by the number of atoms of the molecule under consideration, to give a measure of the stability of the respective compound. Here, the binding energy is defined as the difference of the total energy of the molecule and the combined energy of the atoms fragments constituting the molecule. Table 1 also incorporates data for the indole quinone (IQ) monomer and the most stable dimer, Dimer 3 from Part I of this study.[23]

TABLE 1: Relative Binding Energies for Different Oligomer Sizes

molecule	binding energy per atom (kcal/mol)[a]
IQ[b]	−123.8
Dimer 3[b]	−128.8
tetramer	−140.0
pentamer	−141.4
hexamer	−141.7

[a] Calculated on the BP/DNP level. [b] From ref 23.

Table 1 clearly shows that the system gains more binding energy in the higher oligomers than in the monomers or dimers. If the calculated binding energy/atom is taken as an approximate measure of stability, the chosen tetramer model is ∼16 kcal/mol per atom more stable than the IQ monomer. At higher oligomer sizes, only a small additional amount of binding energy is gained, as the converging values for the binding energies per atom for the pentamer and hexamer structures in Table 1 show.

For the three oligomers, absorption spectra have been calculated using the PECI[35,36] method and the AM1 Hamiltonian,[37] as implemented in the semiempirical program VAMP.[38] The spectra are displayed in Figure 4.

A Lorentzian broadening of 30 nm has been applied to the raw VAMP data, to facilitate comparison with experimental spectra. A discussion of this broadening process can be found in ref 23.

All the spectra show some structure in the visible region of the spectrum. The main absorption peaks are red-shifted with

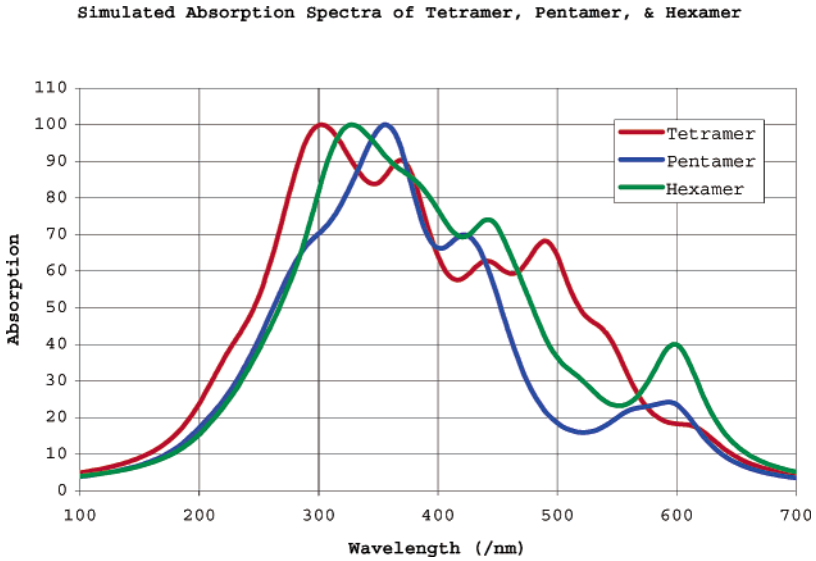

Figure 4. Simulated oligomer absorption spectra. A Lorentzian broadening of 30 nm has been applied to the raw data.

increasing oligomer size. The maximum absorption wavelength, which occurred at 319 nm for the most stable dimer,[23] is ∼370 nm for the tetramer. This peak is shifted in the raw VAMP spectra to ∼420 nm in the pentamer and to ∼440 nm in the hexamer. The difference in red shift between successive oligomers decreases as the oligomer size grows, and from the aforementioned data, it can be expected that the absorption maximum does not shift to wavelengths that are very much higher for larger-sized oligomers.

It is important to note that, for each spectra of Figure 3, (i) the optical peaks that are predicted span the UV, visible, and near-IR region, and (ii) the peaks increase progressively in intensity as the wavelengths decrease.

4. Discussion

One goal of this work is to explain the basis for the broadband optical absorption spectrum of melanin, in terms of its structure. A structural model for melanin has been identified that is based on a series of experimental probes including WAXS,[16,17] STM,[18−20] and SAXS.[21] It is summarized in Figure 2 and consists of 5−7 monomers of IQ and DHI, covalently bonded and arranged in a plane or sheet; the sheets are then drawn together by van der Waal forces and stack 3.4 Å apart, forming a nanometer-sized, graphitic-like layered "protomolecule". We believe that melanin may be considered an aggregate of local structures of ∼3−4 sheets stacked together. For the individual sheets, the polyquinone and polyhydroquinone protomolecules that are held together by hydrogen bonds seem to be acceptable models and represent the experimental data well.[18]

Our calculations indicate that the chosen oligomers yield discrete optical bands. These discrete optical absorption bands have one common feature: an absorption maximum centered at ∼300−370 nm that increases with oligomer size. The newly obtained experimental spectrum (Figure 1) displays a broad absorption feature in this same spectral region, lending credence to the choice of lower-molecular-weight oligomers. During a heterogeneous polymerization, which is believed to occur for melanin, one might expect many additional conformations, alternate to the equilibrium structures calculated in this study. All these various conformations and additional higher- or lower-molecular-weight oligomers will provide absorption bands displaced slightly from these equilibrium structures and could account for the observed smoothness of the experimental

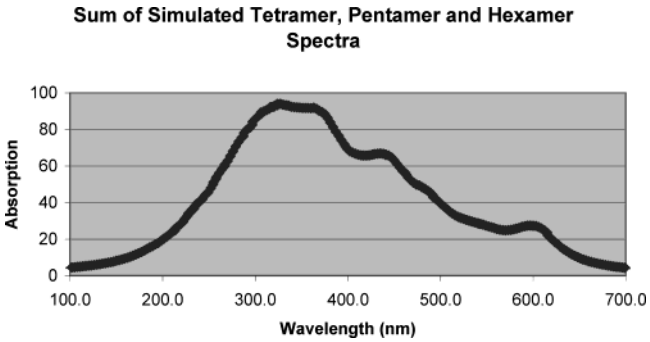

Figure 5. Linear combination of simulated absorption spectra from Figure 4.

eumelanin spectrum. A simple linear combination of the spectra of the oligomers calculated in this study (tetramer, pentamer, and hexamer) is shown in Figure 5. This combination spectrum reproduces some of the important experimental features. The broad absorption maximum centered at ∼300−350 nm is observed; and the monotonic decrease in absorption strength from 300 nm to 800 nm also has been taken into consideration. Thus, our rather simple molecular model is sufficient to account for several salient experimental observations that are well-known in the melanin literature. This agreement argues in favor for this particular structural model over previous higher-molecular-weight models.[7]

The strong absorption at the lowest wavelength for the experimental spectrum of melanin is similar to the behavior of conjugated polymers between dilute solutions and thin films of poly(2-methoxy, 5-(2ethyl-hexoxy)-1,4 phenylene−vinylene (MEH−PPV).[42,43] In those conjugated polymeric systems, it is believed that interchain exciton coupling has an important role in the photoabsorption spectrum, with strong absorption at the lowest wavelength,[44] as is observed in this system. Our simulated one-particle excitation absorption spectrum obtained by semiempirical calculations on a molecular model cannot reflect this many-body effect involving exciton coupling. Therefore, the experimentally observed strong absorption in the high-energy region of the melanin spectrum is absent in the calculated spectra.

The work described here clearly benefits from the recent advance in our knowledge of melanin structure and aggregation behavior and points toward several future steps in the area of

computational physics and chemistry for melanin. We wish to emphasize that, although our calculations are based on state-of-the-art modeling software and theoretical techniques, we are still basing the calculations on a model. In addition, although this structural model has its origin in various experimental investigations, this is still a model for eumelanin and cannot be misconstrued as being verified directly.

On the contrary, the model should be further compared and tested with other physical and chemical properties of melanin besides the optical absorption discussed in this paper. In this way, the model can be further refined and modified, possibly by inclusion of the various moieties known to exist in melanins (such as carboxyl and amine groups and cysteine units), as well as various levels of aggregation of oligomers.

5. Conclusions

The structures of three oligomeric units believed to represent the molecular structure of eumelanins have been optimized using density functional theory. The analysis of the binding energies shows that these subunits are relatively more stable than the substructures with lower molecular weight that have been investigated in Part I of this work.[23]

Absorption spectra of the oligomers have been calculated using semiempirical quantum mechanics techniques. The calculated optical peaks that are predicted span the UV, visible, and near-IR portion of the electromagnetic spectrum, and the peaks progressively increase in intensity as the wavelengths decrease. The lower-molecular-weight oligomers chosen in this study (tetramer, pentamer, hexamer) result in a broad absorption maximum in a spectral region found experimentally. This argues in support for the small oligomeric model that is the focus of the present study. A linear combination of the oligomeric spectra reproduces several features of the experimental spectrum. This result strongly supports the assumption that melanin is constituted of substructures such as those considered in this study.

References and Notes

(1) Chadekel, M. R. *Photochem. Photobiol.* **1982**, *35*, 861.
(2) Giacomoni, P. U. *Photochem. Photobiol. B* **1996**, *29*, 87.
(3) D'Ischia, M.; Napolitano, A.; Prola, G. *Gazz. Chim. Ital.* **1996**, *126*, 783.
(4) Ishii, T. In *Structure and Function of Melanin*; Jimbo, K., Ed.; Fuji, Ltd.: Sapporo, Japan, 1984; pp 43−48.
(5) Kastin, A. J.; Kuzemchak, B.; Tompkins, R. G.; Schally, A. V.; Miller, M. *Brain Res. Bull.* **1976**, *1*, 567.
(6) Young, W. Y. *Surv. Ophthalmol.* **1988**, *32*, 252.
(7) Zeise, L.; Chedekel, M. R.; Fitzpatrick, T. B. *Melanin; Its Role in Human Protection*; Valdnmar Press: Overland Park, KS, 1995.
(8) McGiness, J. E. *Science* **1973**, *177*, 896.
(9) McGiness, J. E. *J. Theor. Biol.* **1973**, *48*, 19.
(10) Proctor, P.; McGiness, J. E.; Corry, P. *Science* **1974**, *183* 853.
(11) Strzelecka, T. *Physiol. Chem. Phys.* **1982**, *14*, 223.
(12) Nicolaus, R. A. *Melanins*; Hermann: Paris, 1968.
(13) Sarna, T.; Swartz, H. A. The Physical Properties of Melanins, *The Pigmentary System: Physiology and Pathophysiology*; Nordlund, J. J. et al. Oxford University Press: New York, 1988; Chapter 25.
(14) Pulman, A.; Pulman, B. *Biochim. Biophys. Acta* **1961**, *54*, 384.
(15) Bolivar-Matinez, L. E.; Galvao, D. S.; Caldas, M. J. *J. Phys. Chem. B* **1999**, *103*, 2993.
(16) Cheng, J.; Moss, S. C.; Eisner, M.; Zschack, P. *Pigm. Cell Res.* **1994**, *7*, 255−262.
(17) Cheng, J.; Moss, S. C.; Eisner, M. *Pigm. Cell Res.* **1994**, *7*, 263.
(18) Zajac, G. W.; Gallas, J. M.; Cheng, J.; Eisner, M.; Moss, S. C.; Alvarado-Swaisgood, A. E. *Biochim. Biophys. Acta* **1994**, *1199*, 271.
(19) Gallas, J. M.; Zajac, G. W.; Sarna, T.; Stotter, P. L. *Pigm. Cell Res.* **2000**, *13*, 99.
(20) Zajac, G. W.; Gallas, J. M.; Alvarado-Swaisgood, A. E. *J. Vac. Sci. Technol. B* **1994**, *12*, 1512.
(21) Gallas, J. M.; Littrell, K. C.; Seifert, S.; Zajac, G. W.; Thiyagarajan, P. *Biophys. J.* **1999**, *77*, 1135.
(22) Stark, K. B.; Gallas, J. M.; Zajac, G. W.; Eisner, M.; Golab, J. T., unpublished work.
(23) Stark, K. B.; Gallas, J. M.; Zajac, G. W.; Eisner, M.; Golab, J. T. *J. Phys. Chem. B* **2003**, *107*, 3061.
(24) Zhang, X.; Erb, C.; Flammer, J.; Nau, W. M. *Photochem. Photobiol.* **2000**, *71*, (5), 524.
(25) Delley, B. *J. Chem. Phys.* **1990**, *92*, 508.
(26) Delley, B. *J. Chem. Phys.* **2000**, *113*, 7756. (DMol^3 is available as part of Materials Studio by Accelrys, Inc.)
(27) Delley, B. In *Density Functional Theory: A Tool for Chemistry*; Seminario, J. M., Politzer, P., Eds.; Elsevier: Amsterdam, The Netherlands, 1995.
(28) Becke, A. D. *J. Chem. Phys.* **1988**, *88*, 2547.
(29) Perdew, J. P. In *Electronic Structure of Solids*; Ziesche, P., Eschrig, H., Eds.; Akademie Verlag: Berlin, p 11.
(30) Perdew, J. P.; Wang, Y. *Phys. Rev. B* **1992**, *45*, 13244.
(31) *Materials Studio DMol^3*, Version 2.1; Accelrys, Inc.: San Diego, CA.
(32) Pulay, P.; Fogarasi, G.; Pang, F.; Boggs, J. E. *J. Am. Chem. Soc.* **1979**, *101*, 2550.
(33) Baker, J.; Kessi, A.; Delley, B. *J. Chem. Phys.* **1996**, *105*, 192.
(34) Andzelm, J.; King-Smith, R. D.; Fitzgerald, G. *Chem. Phys. Lett.* **2001**, *335*, 321.
(35) Clark, T.; Chandrasekhar, J. *Isr. J. Chem.* **1993**, *33*, 435.
(36) Clark, T. In *Recent Experimental and Computational Advances in Molecular Spectroscopy*; NATO ASI Series C; Fausto, R., Ed.; Kluwer Academic Publishers: Dordrecht, The Netherlands, 1993; Vol. 406, p 369.
(37) Dewar, M. J. S.; Zoebisch, E. G.; Healy, E. F.; Stewart, J. J. P. *J. Am. Chem. Soc.* **1985**, *107*, 3902.
(38) Clark, T.; Alex, A.; Beck, B.; Burkhardt, F.; Chandrasekhar, J.; Gedeck, P.; Horn, A.; Hutter, M.; Martin, B.; Rauhut, G.; Sauer, W.; Schindler, T.; Steinke, T. *VAMP*, Version 8.0; University of Erlangen: Erlangen, Germany, 2001. (This version is provided as part of Materials Studio 2.1 by Accelrys, Inc.)
(39) Painter, G. S.; Averill, F. W. *Phys. Rev. B* **1982**, *26*, 1781.
(40) Jones, R. O. *J. Chem. Phys.* **1982**, *76*, 3098.
(41) Johnson, B. G.; Gill, P. M. W.; Pople, J. A. *J. Chem. Phys.* **1993**, *98*, 5612.
(42) Yan, M.; Rothberg, L. J.; Kwock, E. W.; Miller, T. M. *Phys. Rev. Lett.* **1995**, *75*, 1992.
(43) Pichler, K.; Halliday, D. A.; Bradley, D. D. C.; Burn, P. L.; Friend, R. H.; Holmes, A. B. *J. Condens. Matter* **1993**, *5*, 7155.
(44) Yu, Z. G.; Wu, M. W.; Rao, X. S.; Sun, X.; Bishop, A. R. *J. Condens. Matter* **1996**, *8*, 8847.